

A new diagrammatic summation for the effective dielectric response of composites

Rubén G. Barrera, Cecilia Noguez, and Enrique V. Anda

Citation: [The Journal of Chemical Physics](#) **96**, 1574 (1992); doi: 10.1063/1.462141

View online: <http://dx.doi.org/10.1063/1.462141>

View Table of Contents: <http://scitation.aip.org/content/aip/journal/jcp/96/2?ver=pdfcov>

Published by the [AIP Publishing](#)

Articles you may be interested in

[Annealing effect on the dielectric response of novel polymer/nano-quasicrystalline composites](#)

AIP Conf. Proc. **1536**, 879 (2013); 10.1063/1.4810509

[Effect of filament aspect ratio on the dielectric response of multiwalled carbon nanotube composites](#)

J. Appl. Phys. **109**, 094109 (2011); 10.1063/1.3569596

[Effects of orientation and composition on the extrinsic contributions to the dielectric response of relaxor-ferroelectric single crystals](#)

Appl. Phys. Lett. **95**, 142911 (2009); 10.1063/1.3245316

[Dielectric response and tunability of a dielectric-paraelectric composite](#)

Appl. Phys. Lett. **93**, 102908 (2008); 10.1063/1.2982086

[Effective dielectric response of nonlinear composites with external ac and dc electric field](#)

J. Appl. Phys. **95**, 1377 (2004); 10.1063/1.1636260



A new diagrammatic summation for the effective dielectric response of composites

Rubén G. Barrera

Instituto de Física, Universidad Nacional Autónoma de México, Apartado Postal 20-364, 01000 México, Distrito Federal, México

Cecilia Noguez

Instituto de Física, Universidad Nacional Autónoma de México, Apartado Postal 20-364, 01000 México, Distrito Federal, México; and Facultad de Ciencias, UNAM, 04510 México, D.F.

Enrique V. Anda

Instituto de Física, Universidade Federal Fluminense, Outiero de Sao Joao Batista s/n, Centro 24210, Niteroi, Rio de Janeiro, Brasil

(Received 4 April 1991; accepted 11 October 1991)

We extended a previously developed diagrammatic formulation for the calculation of the effective dielectric response of composites prepared as a random, homogeneous, and isotropic distribution of small spherical inclusions in an otherwise homogeneous matrix. This is done within the long-wavelength, dipolar approximation in the low-density regime of inclusions. We propose a new diagrammatic summation and we compare our results with two recently reported computer simulations.

I. INTRODUCTION

The calculation of the effective electromagnetic response of a system composed by an homogeneous matrix with a random, isotropic distribution of small spherical inclusions, has been an active field of research¹ since the pioneering work of Maxwell Garnett² in 1904. The solution found by him, known in the literature as the Maxwell Garnett theory (MGT) is equivalent to the celebrated Clausius-Mossotti-Lorentz-Lorenz relation,³ which links the dielectric response of a fluid with the polarizability and density of its molecules. In the MGT one assumes that in the presence of a long-wavelength external electric field (i) the local field at each inclusion is uniform, thus only the dipolar moment is induced (dipolar approximation) and (ii) that all the spheres acquire exactly the same induced dipole moment, taken equal to its average and calculated self-consistently. This last assumption, which neglects the fluctuations of the induced dipoles, is known as the mean-field approximation (MFA). The relief of these two assumptions has been the challenge which has stimulated the work of many researchers in the last decades.

At low densities of inclusions one expects the dipolar approximation to hold. On the other hand, the MFA breaks down even in the low-density regime, owing to the disorder in the location of the spheres being it the source of the fluctuations. Therefore, it is the tendency towards order that makes the MFA more valid; for example, if the spheres were arranged in the sites of a cubic lattice, all of them would acquire, in the long-wavelength limit, the same induced dipole moment: there would be no fluctuations. In this case the only corrections lacking would be the inclusion of the all the rest of induced multipolar moments.⁴

In this paper our main interest is rather the effects of

disorder, thus our attention will be concentrated in how to improve the MFA, but keeping still the dipolar approximation. There is an ample variety of procedures which have been developed⁵ towards this same goal, but an estimation of their precision through its comparison with experiment has been a painful task. The problem lies in the fact that the experiments performed, up to now, do not resemble properly the models used in the theoretical work. The preparation of homogeneous and isotropic samples, with a well-defined filling fraction of identical spheres, with radius in the nanometer range, has been difficult. Problems like particle clustering, the existence of a distribution of shapes and sizes, and an anomalous high density of dislocations in the small inclusions have obscured a clear interpretation of the effects of disorder in the optical experiments. On the other hand, as pointed out by several authors,⁵⁻¹⁰ beyond MFA the effective dielectric response of a composite depends not only on the filling fraction of the spheres but also on the structure of their two- and three-particle distribution functions. In other words, different types of disorder will lead to different results. Now, since most of the experimentalists do not report the actual distribution functions of the inclusions in their samples, this yields another source of confusion. Fortunately, two numerical simulations of the model used here, also within the dipolar approximation, were recently reported^{11,12} and we have, for the first time, a set of very definite results to test the validity of our theories.

In this work, we develop a new diagrammatic formalism for the calculation of the effective dielectric response of a composite prepared as mixture of identical spheres embedded in an otherwise homogeneous matrix. This formalism is valid only in the low-density regime because of two reasons: (i) the use of the dipolar approximation and (ii) the approximation of the replacement of all the s th particle distribution

functions of the spheres by unsymmetrized products of two-particle distribution functions. After setting up the formalism, we extend a previously performed diagrammatic summation⁸ by including an infinite set of diagrams whose relative importance should be large at low densities. Then we compare our results with the only “experiments” that, we believe, will give the fairest possible comparison: the numerical simulations of Kumar and Cukier,¹¹ and Cichocki and Felderhof,¹² both for a collection of Drude spheres within the dipolar approximation. The structure of the paper is as follows: In Sec. II we develop the diagrammatic formalism and in Sec. III we present a diagrammatic summation which yields a formula similar to one obtained previously with a different procedure. Then, we propose a new diagrammatic summation which can be seen as a vertex decoration of this formula. Our results and their corresponding comparison with the computer simulations are displayed in Sec. IV, while Sec. V is devoted to conclusions.

II. FORMALISM

Let us consider an homogeneous and isotropic ensemble of $N \gg 1$ spheres of radius a and dielectric function ϵ_s , embedded in a host medium with dielectric function ϵ_h . The system is in the presence of a space- and time-dependent external electric field of wave vector \mathbf{q} such that $qa \gg 1$, which oscillates with frequency ω . Under this condition the induced interaction among the spheres can be taken in the quasistatic limit. Within the dipolar approximation, the local electric field at the i th sphere induces an effective dipole moment given by

$$\mathbf{p}_i(\omega) = \alpha(\omega) \left[\mathbf{E}_i^0 + \sum_j \mathbf{t}_{ij} \cdot \mathbf{p}_j \right], \quad (1)$$

where \mathbf{E}_i^0 is the electric field induced in the medium at \mathbf{R}_i , in the absence of the spheres, $\alpha(\omega) = a^3 [\epsilon_m(\omega) - \epsilon_h(\omega)] / [\epsilon_m(\omega) + 2\epsilon_h(\omega)]$ is the effective polarizability of an isolated sphere within the host medium and

$$\mathbf{t}_{ij} = (1 - \delta_{ij}) \nabla_i \nabla_j (1/R_{ij}) \quad (2)$$

is the dipole-dipole interaction tensor (in the quasistatic limit). Here $R_{ij} = |\mathbf{R}_i - \mathbf{R}_j|$ and δ_{ij} is the Kronecker delta.

We excite the system with a longitudinal external field, the polarization is then defined as the average of the induced dipole moment per unit volume which can be related to the effective (or macroscopic) dielectric response $\epsilon_M(\omega)$ of the system through⁵

$$\frac{\epsilon_h(\omega)}{\epsilon_M(\omega)} = 1 - 4\pi\epsilon_h(\omega) \chi^{\text{ex},l}(q \rightarrow 0, \omega), \quad (3a)$$

where $\chi^{\text{ex}}(q, \omega)$ is the external susceptibility defined by

$$n \langle \mathbf{p} \rangle(\mathbf{q}, \omega) = \chi^{\text{ex}}(\mathbf{q}, \omega) \cdot \mathbf{E}^{\text{ex}}(\mathbf{q}, \omega), \quad (3b)$$

and the superscript l denotes longitudinal projection. Here $\mathbf{E}^{\text{ex}}(q, \omega)$ and $\langle \mathbf{p} \rangle(\mathbf{q}, \omega)$ are the Fourier transforms of the external field and the average dipole moment, respectively, n is the number density of spheres, and $\langle \cdots \rangle$ means ensemble average. The fact that the system is excited by a longitudinal rather than a transverse field is just a matter of convenience,

which takes advantage of the fact that in the $q \rightarrow 0$ limit the longitudinal and transverse effective responses coincide. On the other hand, the limiting process ($q \rightarrow 0$) is necessary in order to get around the evaluation of some conditionally convergent integrals.⁵

Lets consider an external field of the form $\mathbf{E}^{\text{ex}} = \hat{\mathbf{q}} E^{\text{ex}} e^{i(\mathbf{q} \cdot \mathbf{r} - \omega t)}$ and then substitute this expression into the equation for the induced dipole moments, Eq. (1), in order to get

$$\mathbf{P}_i = \alpha \left[\frac{\hat{\mathbf{q}} E^{\text{ex}}}{\epsilon_h} + \sum_j \mathbf{T}_{ij} \cdot \mathbf{P}_j \right], \quad (4a)$$

where

$$\mathbf{P}_i = \mathbf{p}_i e^{-i\mathbf{q} \cdot \mathbf{R}_i} \quad \text{and} \quad \mathbf{T}_{ij} = \mathbf{t}_{ij} e^{-i\mathbf{q} \cdot (\mathbf{R}_i - \mathbf{R}_j)} \quad (4b)$$

are so defined in order to get rid of trivial exponential factors and the explicit \mathbf{q} and ω dependence will not be explicitly written from here on. The iterative solution of Eq. (4) was the starting point of the diagrammatic formulation for ϵ_M developed in Ref. 8. One of our objectives here is to recast the diagrammatic series derived in this reference in order to get an alternative series where the diagrams corresponding to the mean-field approximation (MFA) are already summed. For this purpose we rewrite Eq. (4) as

$$\mathbf{P}_i = \alpha(\omega) \left[\mathbf{E}_i^L + \sum_j \Delta \mathbf{T}_{ij} \cdot \mathbf{P}_j \right], \quad (5a)$$

where

$$\mathbf{E}_i^L \equiv \frac{\hat{\mathbf{q}} E^{\text{ex}}}{\epsilon_h} + N \langle \mathbf{T} \rangle \cdot \langle \mathbf{P} \rangle \quad (5b)$$

is known as the Lorentz field, N is the total number of spheres, and

$$\Delta \mathbf{T}_{ij} \equiv \mathbf{T}_{ij} - \langle \mathbf{T} \rangle, \quad (5c)$$

where

$$\langle \mathbf{T} \rangle = \frac{1}{N} \left\langle \sum_j \mathbf{T}_{ij} \right\rangle. \quad (5d)$$

The formal solution of Eq. (5) is

$$\mathbf{P}_i = \alpha \sum_j (\mathbf{V}^{-1})_{ij} \cdot \mathbf{E}^L, \quad (6a)$$

where

$$\mathbf{V}_{ij} \equiv \mathbf{1} \delta_{ij} - \alpha \Delta \mathbf{T}_{ij}, \quad (6b)$$

and $\mathbf{1}$ is the unit tensor. We now define the Lorentz susceptibility as

$$n \langle \mathbf{P} \rangle(q, \omega) = \chi^L(q, \omega) \cdot \mathbf{E}^L(q, \omega), \quad (7)$$

where $\mathbf{E}^L(\mathbf{q}, \omega)$ is the Fourier transform of the Lorentz field. It is easy to show that the effective dielectric response can then be written as

$$\epsilon_M(\omega) = \frac{1 + 2f\tilde{\alpha}\xi}{1 - f\tilde{\alpha}\xi}, \quad (8a)$$

where $f = n4\pi a^3/3$ is the volume fraction of spheres, $\tilde{\alpha} = \alpha/a^3$ and

$$n\alpha\xi = \chi^{L,l}(q \rightarrow 0, \omega) = \lim_{q \rightarrow 0} \left\langle \sum_j (\mathbf{V}^{-1})_{ij}^l \right\rangle. \quad (8b)$$

This equation [Eq. (8a)] has exactly the same functional form as the Maxwell Garnett formula² (or Clausius–Mossotti relation³), except that the bare polarizability $\tilde{\alpha}$ of an isolated sphere is now renormalized by a factor ξ which is proportional to the dipolar response of a sphere to the Lorentz field. The only approximation done, so far, in deriving Eq. (8a) is the dipolar one.

The calculation of the renormalization factor ξ requires the evaluation of the ensemble average of the inverse of matrix \mathbf{V}_{ij} defined in Eq. (6b), which in the thermodynamic limit becomes an infinite matrix with stochastic elements. This is obviously a complicated problem. Here we follow the same method as in Ref. 8 and we use a series representation of the inverse of \mathbf{V}_{ij} in powers of $\Delta\mathbf{T}_{ij}$, given by

$$\sum_j (\mathbf{V}^{-1})_{ij} = 1 + \alpha \sum_j \Delta\mathbf{T}_{ij} + \alpha^2 \sum_{jk} \Delta\mathbf{T}_{ij} \cdot \Delta\mathbf{T}_{jk} + \cdots \quad (9)$$

Then we take an ensemble average assuming that in the low-density regime the s -particle distribution function $\rho^{(s)}(\mathbf{R}_1, \dots, \mathbf{R}_s)$ can be factorized as unsymmetrized sequential products of two-particle distribution functions $\rho^{(2)}(R_{ij})$, i.e.,

$$\rho^{(s)}(\mathbf{R}_1, \dots, \mathbf{R}_s) = \prod_{j=1}^{s-1} \rho^{(2)}(R_{ij}). \quad (10)$$

The end result is a series representation of ξ which can be cast in a diagrammatic form as

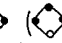
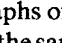
$$\xi = \sum_r \sum_s I(r, s) \equiv o + \text{diagram 1} + \left[\text{diagram 2} + \text{diagram 3} \right] + \left[\text{diagram 4} + \text{diagram 5} + \text{diagram 6} + \text{diagram 7} + \text{diagram 8} + \text{diagram 9} \right] + \cdots, \quad (11)$$

where each diagram is irreducible; this means that it cannot be split into two independent diagrams by cutting a single line. The precise definition of each diagram is given in Ref. 8. Here we will only say that in order to draw a diagram with r lines and s black dots, one starts from a white dot and joins it to all s black dots with r lines, but without lifting the pencil from the paper and without joining a dot to itself. Each line carries a factor α , each black dot carries a factor n , the other factor is an integral over the coordinates of the particles depicted by black dots, being the white dot the reference sphere. The integrand contains the longitudinal projection of the contraction of the propagators \mathbf{T}_{ij} which join the dots i and j weighted by the two-particle distribution functions $\rho^{(2)}(R_{ij})$. For example

$$\begin{aligned} \text{diagram 1} &\equiv n^2 \alpha^3 \lim_{q \rightarrow 0} \int \hat{q} \cdot \mathbf{T}_{12} \cdot \mathbf{T}_{23} \cdot \mathbf{T}_{31} \cdot \hat{q} \\ &\times \rho^{(2)}(R_{12}) \rho^{(2)}(R_{23}) d^3 R_2 d^3 R_3. \end{aligned} \quad (12)$$

One might interpret each diagram as the contribution to the

polarization of a series of elementary processes in which $\alpha\mathbf{T}_{ij}$ propagates the polarization from sphere i to sphere j . The small numbers that appear aside in some of the diagrams of Eq. (11) refer to the order of transversal of the line.

Since a diagram with r lines and s black dots is proportional to $\tilde{\alpha}^r f^s$, its relative importance in the series can be estimated through the relative magnitude of this factor. For example, in the low (high)-density regime the most important diagrams will be those with the smallest (largest) number of dots for a given number of lines; i.e., for four lines a low (high)-density diagram is  (). In Table I we have grouped all the irreducible graphs of lowest order in powers of f and $\tilde{\alpha}$. All the graphs with the same number of black dots (lines) are in the same row (column).

This type of diagrams were already proposed by Hynne,¹³ with exactly the same physical meaning as the one given above, but their incorporation into a formal theory for the calculation of the effective dielectric response was first done in Ref. 8. In this section we have modified this theory in order to get rid of all the nonirreducible graphs. The first application of a diagrammatic method to a composite system was reported by Bergman and Kantor¹⁴ who calculated the effective dc conductivity of a two-component random-resistor network in powers of the conductivity difference of its constituents. Their diagrams look like the ones used here because in both cases a series representation of the inverse of an operator with two-particle interactions was involved.

III. DIAGRAMMATIC SUMMATIONS







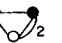



A. Mean-field approximation (MFA)

Since in this new diagrammatic formulation the diagrams which correspond to the MFA are already “summed,” the MFA (or Maxwell Garnett theory) is obtained simply by taking

$$\xi = o = 1. \quad (13)$$

This also means that all the graphs in the series [Eq. (11)] beyond $o (= 1)$ correspond, obviously, to the contributions to the mean polarization coming from the fluctuations of the induced dipole moments around its average value.

TABLE I. Lowest-order irreducible diagrams.

$s \backslash r$	1	2	3	4
1				
2				    
3				

B. Low-density diagrams

Here we choose in the summation all the diagrams with the smallest number of dots (namely two) for a given number of lines. As mentioned above their contribution should be important in the low density regime. In this case we have

$$\xi = o + \text{diagram 1} + \text{diagram 2} + \text{diagram 3} + \text{diagram 4} + \dots \quad (14)$$

Assuming no correlation among the particles beyond the hole correction (HC), $\rho^{(2)}(R) = \Theta(R - 2a)$, where Θ is the unit step function, it is shown in Appendix C of Ref. 8 that this sum yields

$$\xi = 1 + \frac{2}{3} \tilde{f} \alpha \log \left(\frac{8 + \tilde{\alpha}}{8 - 2\tilde{\alpha}} \right). \quad (15)$$

Substituting this expression into Eq. (8a), one obtains an explicit analytic form for the effective dielectric response ϵ_M , which in the limit $\tilde{f} \alpha \ll 1$ becomes

$$\frac{\epsilon_M}{\epsilon_h} = 1 + 3\tilde{f}\alpha + (\tilde{f}\alpha)^2 \left[3 + 2 \log \left(\frac{8 + \tilde{\alpha}}{8 - 2\tilde{\alpha}} \right) \right], \quad (16)$$

which is identical to the expressions obtained in Ref. 8 using a diagrammatic summation and in Ref. 15 using a two-particle cluster integral.

In order to get a deeper insight into the physical interpretation of this approximation we show in Appendix A that one recovers this same expression [Eq. (16)], for ϵ_M if one solves Eqs. (1) directly assuming that a reference sphere interacts with all the other spheres but the rest of them interact only with the reference sphere and not among themselves.

In Fig. 1 we show a plot of $\text{Im } \epsilon_M$ for $f = 0.0217$ and $f = 0.05$ using Eq. (8a) with ξ given by Eq. (15). We chose a system of metallic spheres embedded in dispersionless gelatin with $\epsilon_h = 2.37$. The spheres are described by a Drude dielectric function given by

$$\epsilon_s = 1 - \frac{\omega_p^2}{\omega(\omega + i/\tau)}, \quad (17)$$

where ω_p is the plasma frequency and τ the relaxation time; in Fig. 1 we took $\omega_p \tau = 46$, which is a typical value for a noble metal.

We found that $\text{Im } \epsilon_M$ becomes negative close to the dipolar resonance of the isolated sphere ω_r ($\sim 0.417\omega_p$) whenever $f\omega_p\tau \lesssim 1$, as it can be seen in Fig. 1(b) for $f = 0.05 > 1/46 = 0.0217$. Since $\text{Im } \hat{\alpha}(\omega_r) \sim \omega_p\tau$, one concludes that the approximation proposed in Eq. (14) is inconsistent with the law of increase of entropy whenever $\hat{\alpha} \gtrsim 1/f$. The same problems also appear in Eq. (16) and Felderhof and Jones¹⁶ have proposed a specific healing procedure.

C. A new diagrammatic approximation

In order to avoid the above mentioned limitations, we would require to include diagrams with a larger number of dots for a given number of lines. Thus we propose a new diagrammatic approximation which decorates the series giv-

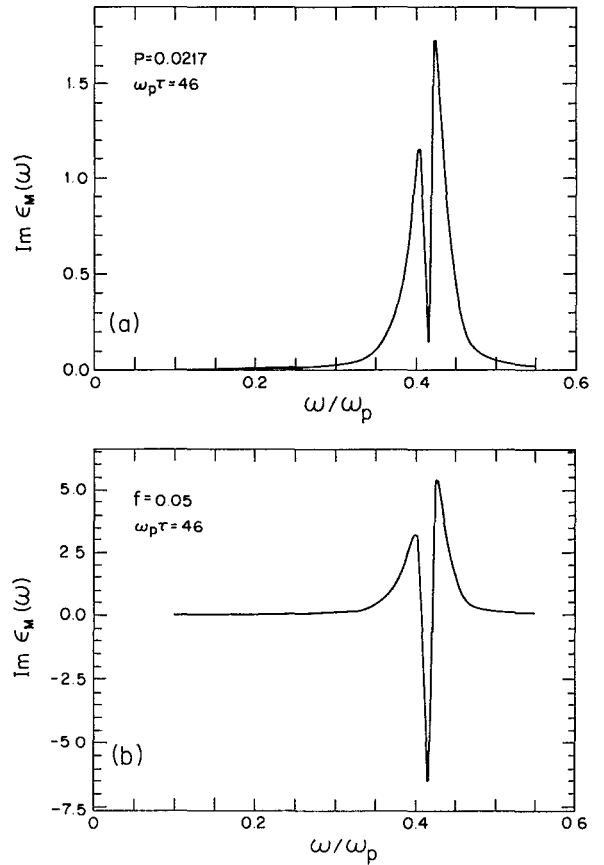


FIG. 1. $\text{Im } \epsilon_M$ as a function of ω/ω_p calculated using Eq. (8a) with ξ given by Eq. (15) for a system of Drude spheres embedded in gelatin. Figures 1(a) and 1(b) correspond to filling fraction of 0.0217 and 0.05, respectively.

en in Eq. (14) by the addition of an infinite class of diagrams. These diagrams corresponds to self-polarization processes which are represented by closed-loop graphs; i.e., processes which starting from a given sphere, polarize the rest of the spheres and finally get back to the initial sphere.

These diagrams include, obviously, graphs with a larger number of dots for a given number of lines, than the ones contained in Eq. (14). The relative importance of these graphs will be evaluated by comparing our results with the ones obtained in recent numerical simulations.^{11,12}

We write

$$\xi = \text{diagram 1} + \text{diagram 2} + \text{diagram 3} + \dots \quad (18a)$$

where the renormalized vertex $\text{diagram 1} \equiv \Delta$ is given by the self-consistent solution of the following diagrammatic equations:

$$\text{diagram 1} = \Delta = o + \text{diagram 4} + \text{diagram 5} + \dots \quad (18b)$$

$$\text{diagram 4} = \eta = \text{diagram 6} + \text{diagram 7} + \text{diagram 8} + \dots \quad (18c)$$

A few examples of the graphs included in ξ are, for instance,


(19)

We also assume that the graphs η which appear in Eq. (18b) are statically independent, thus

$$\Delta = 1 + \eta + \eta^2 + \eta^3 + \cdots = \frac{1}{1 - \eta}. \quad (20)$$

A more restricted approximation consists in taking simply

$$\xi = \Delta \quad \text{and} \quad \eta = , \quad \text{(21)}$$


which corresponds to the approximation developed in Ref. 8 [see Eq. (27)] and known as renormalized polarizability theory (RPT).⁵

In order to calculate η we first define the tensor Δ such that $\Delta = \hat{q} \cdot \Delta \cdot \hat{q}$. Now, instead of taking the longitudinal projection of the contraction first and then the average, we first perform the tensorial contraction, take 1/3 of its trace and then average; this will give the same result due to the isotropy of the ensemble with $\Delta = \mathbf{I}\Delta$.

The equation for η [Eq. (18c)] can then be written as

$$\eta = \frac{1}{3} T_r \left\{ \left\langle \sum_j \mathbf{T}_{ij} \cdot \Delta \cdot \mathbf{T}_{ji} \right\rangle + \left\langle \sum_j \mathbf{T}_{ij} \cdot \Delta \cdot \mathbf{T}_{ji} \cdot \mathbf{T}_{ij} \cdot \Delta \cdot \mathbf{T}_{ji} \right\rangle + \cdots \right\} \quad (22a)$$

$$= \frac{1}{3} T_r \left\{ \left\langle \sum_j \mathbf{T}_{ij} \cdot \Delta \cdot \mathbf{T}_{ji} \cdot (1 - \mathbf{T}_{ij} \cdot \Delta \cdot \mathbf{T}_{ji})^{-1} \right\rangle \right\}, \quad (22b)$$

which yields finally

$$\eta = 4\pi n \alpha^2 \Delta \left[\int_0^\infty \frac{\rho^{(2)}(R)}{R^4 (1 - \alpha^2 \Delta / R^6)} dR + \int_0^\infty \frac{\rho^{(2)}(R)}{R^4 (1 - \alpha^2 \Delta / R^6) (1 - 4\alpha^2 \Delta / R^6)} dR \right]. \quad (23)$$

Following the same procedure we calculate ξ summing all the diagrams which appear in Eq. (18a) and we get

$$\xi = 8\pi n \alpha^3 \Delta^4 \int_0^\infty \frac{\rho^{(2)}(R)}{R^7 (1 - \alpha^2 \Delta^2 / R^6) (1 - 4\alpha^2 \Delta^2 / R^6)} dR. \quad (24)$$

We assume that the two-particle distribution function is given by the $\rho_{\text{HC}}^{(2)} = \Theta(R - 2a)$, which should be valid in the low-density regime. Then, the integrals [Eqs. (23) and (24)] can be performed analytically and we obtain

$$\xi = \Delta + \frac{1}{3} f \alpha \Delta^2 \log \left(\frac{64 - \tilde{\alpha}^2 \Delta^2}{64 - 4\tilde{\alpha}^2 \Delta^2} \right), \quad (25a)$$

where Δ is given by the self-consistent solution of the following equation:

$$\Delta = \left[1 - \frac{1}{3} f \alpha \sqrt{\Delta} \log \frac{(4 + \tilde{\alpha} \sqrt{\Delta})(8 + \tilde{\alpha} \sqrt{\Delta})}{(4 - \tilde{\alpha} \sqrt{\Delta})(8 - \tilde{\alpha} \sqrt{\Delta})} \right]^{-1}. \quad (25b)$$

IV. RESULTS

We now show our results for a system of Drude spheres embedded in vacuum with $\omega_p \tau = 94$. We chose this particular system in order to compare our results with the numerical simulations recently reported by Kumar and Cukier,¹¹ for $f = 0.01$; 0.03 ; and 0.1 . In this work, periodically repeated configurations of 48 spheres within a cube were generated for a hard-sphere fluid in equilibrium. The polarization averages were taken over 500 configurations on spherical regions which contained about 25 spheres, on the average. In Fig. 2 we plot $\text{Im} \epsilon_M$ as a function of ω/ω_p for $f = 0.01$; 0.03 ; and 0.1 . The continuous lines are our theoretical results and the dots are the results of the numerical simulation taken directly from the paper of these authors. One can see that for $f = 0.01$ and $f = 0.03$ we have an excellent agreement between our results and the ones of the numerical simulation. One should add that these results deviate appreciably from the ones predicted by the MFA, as discussed in Kumar and Cukier's work.¹¹ This clearly means that the infinite class of diagrams that we have chosen are those which become more important in the low-density regimen. For $f = 0.1$ the agreement is not exact but is obviously very good.

Using the same numerical simulation procedure and the same system of Drude spheres, Cukier *et al.*¹⁷ have also studied the changes in the profile of the absorption peak, in $\text{Im} \epsilon_M(\omega)$, for different types of disorder. They have generated distinct classes of configurations, with different algorithms which weight differently the probability of finding a sphere around the positions of an ordered system, and they find noticeable changes in the profile of the peak. In our theory those changes should arise from different choices of the two-particle distribution function. Unfortunately this information is not reported, thus a further comparison of our theoretical results with their numerical simulations is not possible now.

Another numerical simulation has been reported by Cichocki and Felderhof¹² who display their results in terms of the spectral function $g(u)$. This function, introduced by Bergman,¹⁸ is defined through the following integral representation of ϵ_M :

$$\frac{\epsilon_M}{\epsilon_h} = 1 - f \int_0^1 \frac{g(u)}{t - u} du, \quad (26)$$

where the variable t is defined by

$$t = \frac{1}{1 - \epsilon_s/\epsilon_h}. \quad (27)$$

The main advantage of this representation is that $g(u)$ does not depend on the dielectric properties of the materials

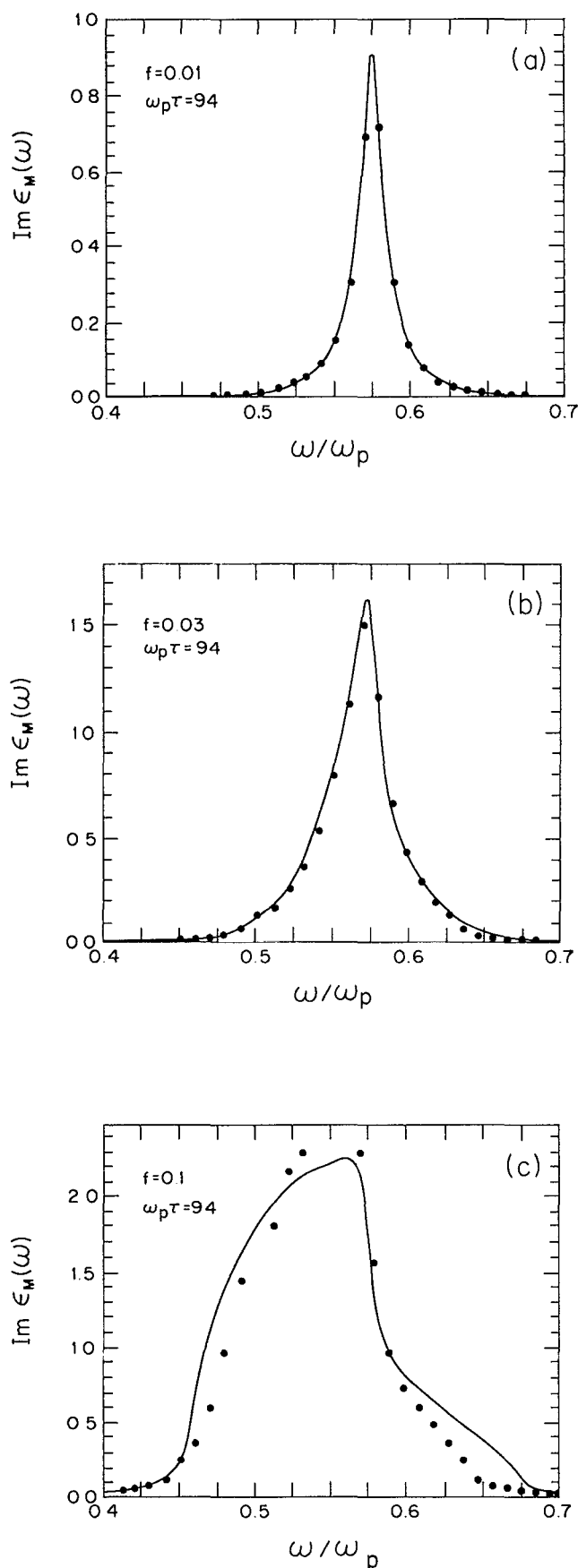


FIG. 2. $\text{Im } \epsilon_M$ as a function of ω/ω_p for filling fractions 0.01 (a), 0.03 (b), and 0.1 (c). The solid line corresponds to Eq. (8a) with ξ given by Eq. (25) and the dots are the results of the computer simulation of Ref. 11.

which compose the system. It is essentially a property of the geometry and the spatial distribution of the inclusions and it measures the weight of the normal electromagnetic modes of the system. For example, in our system, the MFA yields $g(u) = \delta[u - 1/3(1-f)]$ because in the absence of fluctuations and in the long-wavelength limit, only one mode can be excited.

Cichocki and Felderhof performed their computer simulations at six volume fractions (0.1; 0.2; 0.3; 0.4; 0.4618; and 0.5). At each volume fraction the average was taken over N_x independent configurations generated earlier in a Monte Carlo simulation of the hard sphere system in equilibrium. The configurations considered N_c particles within a cube which was then repeated periodically. Since our theory is valid only in the low density regime here we compare our results only for the three lowest filling fraction used by Cichocki and Felderhof. For these filling fractions, they have taken $N_c = 300, 500$, and 580 and $N_x = 500, 250$, and 200 , respectively.

In Fig. 3 we plot $g(u)$ as a function of u for $f = 0.1; 0.2$; and 0.3 . The dotted lines are the results of the computer simulation and the continuous lines are our theoretical results. The dashed lines are calculated using the RPT theory, given here by Eq. (21). It can be readily seen that for $f = 0.1$ we have a very good agreement between our theory and the computer-simulation results. For $f = 0.2$, although the agreement is not as good, the main features of the shape of the profile are maintained. For $f = 0.3$ the peak in our theory is redshifted, higher, and more asymmetric than the computer-simulation result. It is not surprising that for such high filling fractions our approximations, in particular the factorization of the s -particle distribution function [Eq. (10)], starts to break down. It is also interesting to notice that for $f = 0.3$ our results start to resemble the ones given by RPT. This resemblance is even greater for $f = 0.4$ and 0.5 (not shown here) which clearly reflects, that in Eq. (18), all the graphs with more than two lines between vertexes will not be important in the high-density regime. Another distinctive feature of our results is an extremely deep and sharp minimum at $u = 1/3$. Since the resonance of the isolated sphere is, precisely, at $u = 1/3$, this means that our approximation is not able to handle very large values of α .

V. CONCLUSIONS

We have derived a new diagrammatic series for the calculation of the effective dielectric response of a composite made up of identical spheres embedded in an otherwise homogeneous matrix. The series is valid for low filling fractions of spheres and its zeroth-order term is already the mean-field approximation; this means that all the graphs in the series represent elementary-polarization processes corresponding to fluctuations around the mean polarization.

The summation of extreme low-density graphs was performed and it was shown that in a certain limit this expression was identical to the one derived by a two-cluster expansion. A different way of deriving this expression, which showed very clearly its physical meaning, was also presented and its shortcomings were discussed. A new diagrammatic

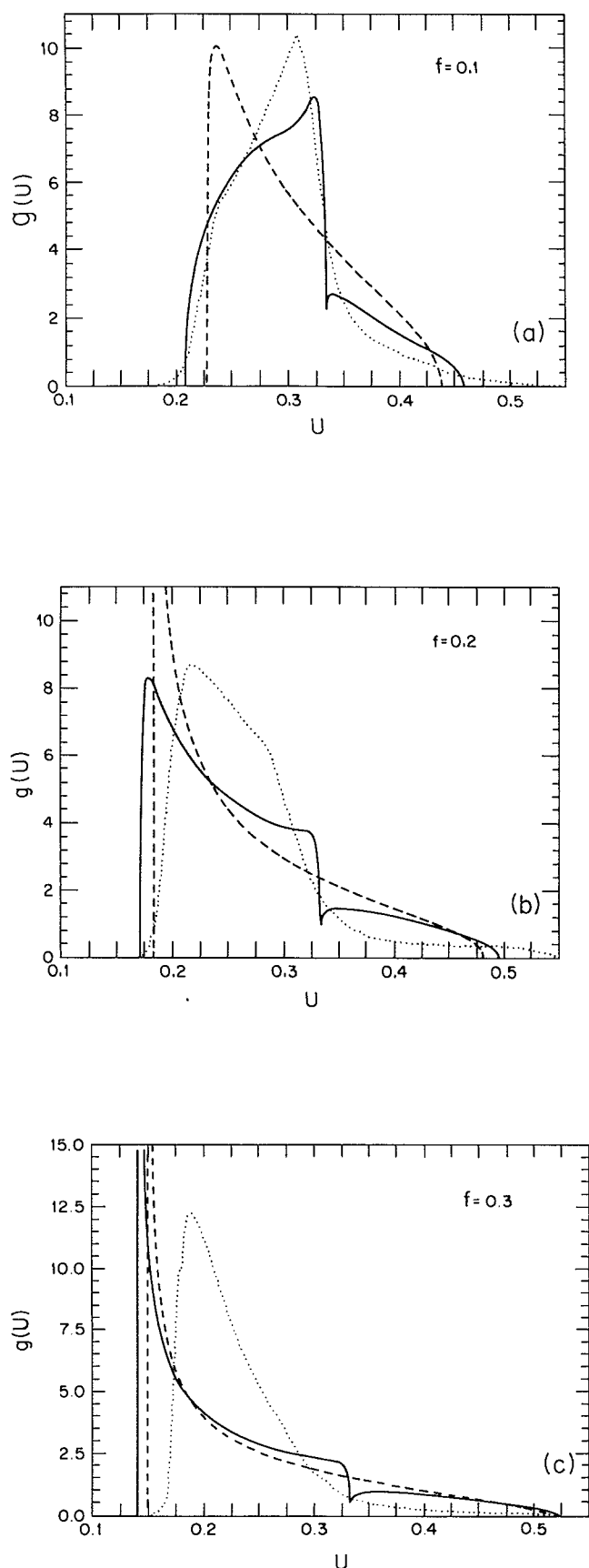


FIG. 3. The spectral function $g(u)$ as a function of u for filling fraction 0.1 (a), 0.2 (b), and 0.3 (c). The solid (broken) line corresponds to Eq. (8a) with ξ given by Eq. (25) [Eq. (21)]. The dotted line is the computer simulation of Ref. 12.

approximation was then proposed and its results were compared with two recently developed numerical simulations. We found an excellent agreement between our results and the ones given by the computer simulations, for filling fractions $f \leq 0.1$.

ACKNOWLEDGMENTS

We are pleased to acknowledge very stimulating discussions with W. Luis Mochán, Guillermo Monsivais, and Marcelo del Castillo. R.G.B. and E.V.A. would like to acknowledge the kind hospitality of Instituto de Física of the Universidade Federal Fluminense and Instituto de Física of the Universidad Nacional Autónoma de México, respectively. This work was partially supported by Proyecto DGAPA IN-104689 of Universidad Nacional Autónoma de México (México), Conselho Nacional de Desenvolvimento Científico e Tecnológico, CNPq (Brazil), and Financiadora de Estudos e Projetos FINEP (Brazil).

APPENDIX A

In this Appendix we derive Eq. (15) by solving directly Eqs. (1) under specific approximations. We start with

$$\mathbf{p}_i = \alpha \left[\mathbf{E}^0 + \sum_j \mathbf{t}_{ij} \cdot \mathbf{p}_j \right], \quad (1)$$

where \mathbf{E}^0 is the electric field induced in the absence of the spheres, and it is assumed constant in space.

We then choose a reference sphere located at \mathbf{R}_0 interacting with the rest of the N spheres, thus its induced dipole moment is given by

$$\mathbf{p}_0 = \alpha \left[\mathbf{E}^0 + \sum_j^N \mathbf{t}_{0j} \cdot \mathbf{p}_j \right]. \quad (A1)$$

It is now assumed that the rest of the spheres interact only with the reference sphere but not among themselves, i.e.,

$$\mathbf{p}_j = \alpha [\mathbf{E}^0 + \mathbf{t}_{j0} \cdot \mathbf{p}_0]. \quad (A2)$$

Substituting this equation into the equation for the induced dipole moment of the reference sphere [Eq. (A1)] yields

$$\mathbf{p}_0 = \alpha \mathbf{E}^0 \left[\mathbf{1} + \sum_j^N \alpha \mathbf{t}_{0j} \cdot (\mathbf{1} - \alpha \mathbf{t}_{0j})^{-1} \right], \quad (A3)$$

where $\mathbf{1}$ is the unit dyadic. The explicit calculation of the right-hand side of Eq. (A3) gives immediately

$$\mathbf{p}_0 = \alpha \mathbf{E}^0 \cdot \left[\mathbf{1} + \sum_j^N \frac{\alpha/R_{0j}^3 (3\hat{\mathbf{R}}_{0j}\hat{\mathbf{R}}_{0j} - \mathbf{1}) + 2\alpha^2/R_{0j}^6 \mathbf{1}}{(1 + \alpha/R_{0j}^3)(1 - 2\alpha/R_{0j}^3)} \right]. \quad (A4)$$

Since $\langle \mathbf{p}_0 \rangle$ is along \mathbf{E}_0 , due to the isotropy of the ensemble, one is able to calculate $\langle \mathbf{p}_0 \rangle$ by taking the average of $1/3$ of the trace of the tensor in brackets in the right-hand side of Eq. (A4). This gives

$$\langle \mathbf{p}_0 \rangle = \alpha \mathbf{E}^0 \left[1 + 8\pi n \int_0^\infty \frac{\alpha^2/R^6}{(1 + \alpha/R^3)(1 - 2\alpha/R^3)} \times \rho^{(2)}(R) R^2 dR \right]. \quad (A5)$$

Substitution of $\rho^{(2)}(R) = \Theta(R - 2a)$ into Eq. (A5) yields, by direct integration,

$$\langle p_0 \rangle = \alpha E^0 \left[1 + \frac{8\pi}{3} n\alpha \log\left(\frac{8 + \alpha}{8 - 2\alpha}\right) \right]. \quad (\text{A6})$$

Since in the low-density limit $E^0 \simeq E^{\text{ex}} \simeq E^L$, the renormalization factor of α is given by the expression in brackets in Eq. (A6) which is the same as Eq. (15).

- ¹ See, for example, *Electrical Transport and Optical Properties of Inhomogeneous Media*, AIP Conference Proceedings, edited by J. C. Garland and D. B. Tanner (American Institute of Physics, New York 1978); *Electrodynamics of Interfaces and Composite Systems*, Advanced Series in Surface Science, Vol. 4, edited by R. G. Barrera and W. L. Mochán (World Scientific, Singapore, 1988); *ETOPIM 2, Proceedings of the Second International Conference on Electrical Transport and Optical Properties of Inhomogeneous Media*, edited by J. Lafait and D. B. Tanner (North Holland, Amsterdam, 1989).
- ² J. C. Maxwell Garnett, *Philos. Trans. R. Soc. London* **302**, 385 (1904).

- ³ *Classical Electrodynamics*, 2nd ed., edited by J. D. Jackson (J. Wiley, New York, 1975), Sec. 4.5.
- ⁴ See, for example, W. T. Doyle, *J. Appl. Phys.* **49**(2), 795 (1978); R. C. McPhedran and D. R. McKenzie, *Proc. R. Soc. London, Ser. A* **359**, 45 (1978); L. Polodian and R. C. McPhedran, *ibid.* **408**, 45 (1986).
- ⁵ See, for example, R. G. Barrera, G. Monsivais, and W. L. Mochán, *Phys. Rev. B* **38**, 5371 (1988), and references there in.
- ⁶ V. A. Davis and L. Schwartz, *Phys. Rev. B* **31**, 5155 (1985); **33**, 6627 (1986).
- ⁷ B. U. Felderhof, *J. Phys. C* **15**, 1731, 3943, 3953 (1982); *Physica A* **126**, 430 (1984).
- ⁸ R. G. Barrera, G. Monsivais, W. L. Mochán, and E. Anda, *Phys. Rev. B* **39**, 9998 (1989).
- ⁹ S. Torquato and F. Lado, *Proc. R. Soc. London, Ser. A* **417**, 59 (1988).
- ¹⁰ L. Tsang and J. A. Kong, *J. Appl. Phys.* **53**, 7162 (1982).
- ¹¹ S. Kumar and R. I. Cukier, *J. Phys. Chem.* **93**, 4334 (1989).
- ¹² B. Cichocki and B. U. Felderhof, *J. Chem. Phys.* **90**, 4960 (1989).
- ¹³ F. Hynne, *Am. J. Phys.* **51**, 837 (1983).
- ¹⁴ D. J. Bergman and Y. Kantor, *J. Phys. C* **14**, 3365 (1981).
- ¹⁵ B. U. Felderhof, G. N. Ford, and E. G. D. Cohen, *J. Stat. Phys.* **28**, 135 649 (1982).
- ¹⁶ B. U. Felderhof and R. B. Jones, *Z. Phys. B* **62**, 43 (1985); **62** 215, 225 (1986).
- ¹⁷ R. I. Cukier, J. Karkheck, S. Kumar, and S. Y. Sheu, *Phys. Rev. B* **41**, 1630 (1990).
- ¹⁸ D. J. Bergman, *Phys. Rep.* **43**, 377 (1978).